Ni/Al Layered Double Hydroxide and Carbon Nanomaterial composites for Glucose Sensing

Ni/Al Layered Double Hydroxide and Carbon Nanomaterial Composites for Glucose Sensing

*Isacco Gualandi†, Ylea Vlamidis†, Lorenzo Mazzei†, Elisa Musella†, Marco Giorgetti†, Meganne Christian‡, Vittorio Morandi‡, Erika Scavetta†, Domenica Tonelli†**

†Dipartimento di Chimica Industriale 'Toso Montanari', Università di Bologna, Viale Risorgimento 4, 40136 Bologna, Italy

‡Istituto per la Microelettronica e i Microsistemi (IMM), Consiglio Nazionale delle Ricerche (CNR), Sede di Bologna, via Gobetti 101, 40129 Bologna, Italy

KEYWORDS**:** layered double hydroxide, carbon nanotubes, graphene, glucose sensor, composite material

ABSTRACT: Layered double hydroxides (LDHs) have been combined with graphene and/or carbon nanotubes to prepare new composite materials with fascinating electrochemical features. For the first time, this work describes the development of an electrosynthesis protocol that allows the deposition of thin films of a Ni/Al LDH on glassy carbon electrodes previously modified with carbon nanomaterials. Three different approaches (potentiostatic, galvanostatic and potentiodynamic) were investigated in order to identify the best procedure. In all cases the potentiodynamic synthesis exhibits better reproducibility than the potentiostatic one which is the most used in literature. The reliability of the synthesis protocol was evaluated by performing the LDH electrodeposition using glassy carbon electrodes modified with multiwalled carbon nanotubes and/or electrochemically reduced graphene oxide arranged in five configurations. XRD and SEM analysis confirmed the LDH formation. Cyclic voltammetry shows the graphene presence ensured a large electrochemically active area with values 3 times higher than the one observed for an LDH deposited on a bare glassy carbon.

Moreover, impedance electrochemical spectroscopy highlights that carbon nanomaterials play a key role in reducing the charge transfer resistance. In fact, it decreases from 2800 KΩ recorded for LDH deposited on bare glassy carbon to about 600 Ω for the best composite material. The materials were tested for glucose electrooxidation which was exploited for the fabrication of a sensor with high sensitivity (2.6 A M^{-1} cm^{-2} for the best device) and low limit of detection (0.6 μM for the best device).

1. INTRODUCTION

Nanomaterials are playing a key role in the design of new electrochemical devices that could have a huge impact on people during everyday life. The processes that involve electricity and chemical change underpin the direct conversion of electrical to chemical energy and vice versa and can be exploited in several systems for energy storage and production, such as supercapacitors[1,2], batteries[3,4], solar[5] and fuel cells[6,7]. These systems play a key role in the fabrication of portable electronic devices and in the development of a renewable energy grid. On the other hand, electrochemical reactions offer a very quick, cheap and simple transduction of chemical signals[8]. In fact, several commercial glucose sensors take advantage of these features to measure daily the glycemia of millions of diabetic patients around the world[4]. The commercialization of new portable devices for other biomarkers would enhance the point-of-care medical service with a general improvement of quality of life.

Layered double hydroxides (LDHs) are a promising class of materials that is widely employed in the above-cited fields because they offer exciting electrochemical features[9–11]. LDHs, also known as hydrotalcite-like compounds, are synthetic anionic clays belonging to the group of brucite-like layered materials. The LDH general formula is $[M^{2+}_{1-x}M^{3+}_{x}(OH)_2]^{x+}(A^{n-})_{x/n}$ m H_2O, where M^{2+} and M^{3+} are divalent and trivalent cations that are tetrahedrally or octahedrally coordinated to form two-dimensional layers that exhibit a positive charge[12]. Consequently, anions (A^{n-}) are intercalated into the interlayer region to maintain the electroneutrality of the material. The LDH features can be tuned by varying their chemical composition because a wide spectrum of metal cations can be used as M^{2+} (Mg^{2+}, Ni^{2+}, Co^{2+}, Cu^{2+}, Mn^{2+} or Zn^{2+}) and M^{3+} (Al^{3+}, Fe^{3+}, Cr^{3+} or Ga^{3+}) and different anions can be

intercalated in the interlayer to finely control the distance between the brucite sheets[13]. Besides the tunability of the composition and structure, LDHs are attractive because of their large active area and their ability to exchange and preconcentrate anions.

Redox-active LDHs can be produced using transition metals such as Co, Ni and Mn which can undergo a Faradaic reaction in a useful potential range[14]. The materials obtained can conduct electricity due to electron hopping between metal centers that are close together and ionic displacement inside or outside the material, even though their conductivity is not very high. The charge and discharge processes involving redox active centers can be exploited to store electrical energy and, for this reason, conductive LDHs have been proposed as pseudo capacitive materials to produce supercapacitors[15]. Furthermore, the redox metal can promote Faradaic reactions through electrocatalytic pathways which are used for different purposes, such as amperometric sensors[16], anodes in fuel cells[17,18], and for electrochemical water oxidation[19,20].

Nevertheless, many LDH applications are still largely restricted because of: 1) low electrical conductivity that reduces the performance of electrochemical devices when high current densities flow in the material[14,21]. This feature is a key point in supercapacitor applications due to the high currents flowing during fast charge-discharge cycles. The same is true for the oxygen evolution reaction to guarantee a fast rate of the process; 2) performance decay during device operation due to the volume change associated with a variation of the redox state of the material[21].

These weak points can be overcome by combining LDHs with carbon nanomaterials in the form of carbon nanotubes (CNTs)[14,22,23] and graphene (G), usually obtained by the reduction of graphene oxide[13,24]. CNTs and G are different allotropes of carbon. CNTs are cylindrical with a length significantly greater than the other dimensions[25]. G is a single layer of carbon atoms arranged in a hexagonal lattice[26]. Both materials exhibit high accessible surface area, good electrical conductivity, chemical and thermal stability, and mechanical strength. Nevertheless, CNTs and G display a low electrochemical reactivity and their polarization takes place through the double layer charging with

an associated capacity that is remarkably lower than that of LDH materials. Furthermore, they have a negative surface charge due to the presence of oxygenated functional groups.

Therefore, LDHs and carbon nanomaterials have complementary properties. Several LDH/graphene and LDH/CNT composite materials were synthesized by bulk chemical synthesis[27] or assembled by exploiting the opposite charge of carbon nanomaterials and brucite layers[28]. The resulting composites take advantage of the intrinsic conductivity of carbon nanomaterials and superior electrochemical features of LDHs to obtain a synergistic effect that remarkably boosts their electrochemical performance. Moreover, the complementary structure of the two components hinders or slows LDH reorganization processes that take place during the working of the electrochemical devices based on LDHs thus leading to an inadequate operational stability for real life applications[21,29].

Since the LDH/carbon nanomaterials composites are usually synthesized by bulk techniques (urea hydrolysis and co-precipitation, solvothermal and hydrothermal methods), several steps must be performed to prepare the final electrochemical devices. First, the material must be separated from the synthesis solution and the solid composite nanomaterial is usually dispersed with a binder (polytetrafluoroethylene, acetylene black or Nafion®) in order to obtain a suspension. Then a small volume is deposited on the electrode surface and the modifying film is attained after drying. In addition to this tedious procedure, the drop casting electrode preparation leads to a little control over the film thickness and a poor adhesion between the modifier and the electrode.

Alternatively, the modification of any conductive surface can be performed by electrosynthesis with a protocol developed by Tonelli's group[30,31]. The thin films obtained have been extensively investigated for different applications that include amperometric sensors[16], supercapacitors[32], anodes for fuel cells [18], the oxygen evolution reaction[20] and the development catalysts for heterogeneous gas-phase reactions [33]. Electrosynthesis takes advantage of the reduction of nitrate and water at cathodic potential to quickly and cheaply precipitate the LDH on the surface of the conductive support. Moreover, this approach can be easily applied for the direct modification of porous surfaces which

are proposed as electrode materials with large surface area, that is a key point in several real applications. Electrochemical deposition usually needs few minutes to be accomplished[16,18,20,31,32,34], therefore it is faster than the chemical synthesis that usually requires at least hours[14,21–23,27,28,35–42] considering both the addition of the reagent and the time wherein the precipitate is kept in contact with mother liquor. Therefore, during the electrochemical deposition the material does not have time to reorganize its structure and it generally exhibits a low crystallinity[31]. In addition, our previous study demonstrated that the extent of LDH crystallinity depended also on the kind of conductive support[30].

The aim of this work is the development of an electrosynthesis protocol that allows the preparation of nanostructured films by the deposition of a Ni/Al based LDH on carbon nanomaterial films in order to produce a new electrochemical interface that takes advantage of the unique properties of both materials. Ni/Al LDH has been chosen because it can conduct electricity and offers a well-reproducible redox behavior that can be exploited for several applications. The nanomaterials are multiwalled carbon nanotubes (MWCNTs) and/or graphene oxide (GO) which are also mixed together to obtain different configurations as described by Sharma et al. (2017)[43]. Five different interfaces are considered in this work to demonstrate the reliability of the proposed approach and the superior performances have been demonstrated by electrochemical impedance spectroscopy and using the modified electrode for glucose detection. To the best of our knowledge, it is the first example of LDH electrochemical synthesis performed on carbon nanomaterials.

2. EXPERIMENTAL

2.1 Reagents and apparatus

Aqueous GO solution (4 mg ml^{-1}), MWCNTs (O.D. × wall thickness × L = 20-30 nm × 1-2 nm × 0.5-2 μm), lithium perchlorate, aluminium nitrate, nickel nitrate and sodium hydroxide were obtained from Sigma-Aldrich. All chemicals were of analytical reagent grade and were used as received,

without further purification. All aqueous solutions were prepared with doubly distilled (DD) water with the exception of the MWCNTs which were suspended in N,N-dimethyl formamide (DMF, 2 mg ml^{-1}). The suspension was submitted to ultrasonic treatment for 20 min at 40% maximum power using a Bandelin Sonorex Super Sonicator (RK 103 H).

The electrochemical experiments were performed with a potentiostat/galvanostat electrochemical workstation PGSTAT20 (Metrohm, The Netherlands) interfaced with a personal computer. A three-electrode conventional electrochemical cell was employed, with a 3 mm diameter GCE from BASi as the working, a saturated calomel electrode (SCE) as the reference and a Pt wire as the counter electrode.

Scanning Electron Microscope (SEM) observations were performed with a ZEISS Leo 1530 microscope equipped with a Schottky emitter, operated at 5 keV and collecting secondary electrons by means of an In-Lens detector. The samples were observed without additional metallization, except for the cross-section of the "blank" glassy carbon electrode, in which case a sputtered coating of gold was used to render it more conductive for imaging purposes. Energy Dispersive X-ray Spectroscopy measurements were performed using the integrated Oxford 30 mm^2 Silicon Drift Detector.

2.2 Preparation of the chemically modified electrode

Prior to the electrochemical measurements, the GC surface was gently polished on wet (4000 grit) SiC sand paper until a mirror finish was obtained. Then it was thoroughly rinsed with DD water and left to dry at room temperature.

A scheme of the electrochemical modification is shown in Fig 1 A. The chemically modified electrode was prepared by drop casting the carbon nanomaterials (GO or MWCNTs) directly onto the GC surface. Different amounts of GO and MWCNTs were tried in order to prepare the chemically modified electrodes (CMEs). Five different configurations were tested as shown below, indicating the carbon nanomaterial(s) used, and the deposition order in the case of the bilayers:

1-only GO (named ERGO/GC after electrochemical reduction): the electrode was prepared by drop casting 10 µL of 0.2 mg mL^{-1} GO.

2-only MWCNTs (MWCNTs/GC): the electrode was prepared by drop casting 10 µL of 0.6 mg mL^{-1} MWCNTs.

3-Bilayer MWCNTs/GO (Bilayer1/GC): after drop casting 7 µL of 0.6 mg mL^{-1} MWCNTs solution (drying for 15 min at 60°C), 10 µL of 0.2 mg mL^{-1} GO were deposited.

4-Bilayer GO/MWCNTs (Bilayer2/GC): after drop casting 10 µL of 0.2 mg mL^{-1} GO solution (drying for 15 min at 60°C), 7 µL of 0.6 mg mL^{-1} MWCNTs were deposited.

5-Composite GO-MWCNTs (Composite/GC): the electrode was prepared by drop casting 10 µL of a solution containing 0.2 mg mL^{-1} GO and 0.2 mg mL^{-1} MWCNTs.

The thicknesses of nanomaterial films were controlled by the volume and the concentration of GO and MWCNTs in the deposition solution. In each case, after casting a carbon nanomaterial the electrodes were dried at 60 °C in an oven for 15 min. After that, all the modified electrodes were submitted to 10 CV cycles between 0 and −1.3 V in order to convert GO to electrochemically reduced graphene oxide (ERGO).

Different experimental approaches were employed to perform the LDH electrochemical syntheses in a solution containing 22.5 mM $Ni(NO_3)_2$ and 7.5 mM $Al(NO_3)_3$:

- Potentiostatic deposition: the LDHs films were deposited by applying at the electrodes -1.1 V for 30 s.
- Galvanostatic deposition: the electrosynthesis was carried out in 5 steps in which a current of -0.5 mA was applied for 5 s. Between every cathodic pulse, a zero current step was performed for 5 s.

- Potentiodynamic deposition: the LDH was deposited by CV from 0 to -1.35 V (2 cycles at the scan rate of 0.010 V s^{-1})

The procedures employed for potentiodynamic and galvanostatic depositions were optimized after a preliminary investigation that was devoted to obtain the highest reproducibility. On the other hand, we employed the procedure already described in literature for the potentiostatic deposition. The electrodes modified with LDH films are named LDH/GC, LDH/ERGO/GC, LDH/MWCNTs/LDH, LDH/Bilayer1/GC, LDH/Bilayer2/GC and LDH/Composite/GC if they are obtained from an electrosynthesis on bare GC, ERGO/GC, MWCNTs/GC, Bilayer1/GC, Bilayer2/GC and Composite/GC, respectively. The LDH structure from potentiodynamic synthesis was verified by collecting X-ray diffraction patterns using CuKa radiation in reflection mode by means of an X'Pert PANalytical diffractometer equipped with a fast X' Celerator detector.

2.3 Electrochemical characterization

2.3.1 Determination of electrochemically active surface area (ECSA)

The electrochemically active areas were estimated using the approach proposed by McCrory et al.[44] in 1 M NaOH. The method estimates the double-layer capacitance of the system from CV, by measuring the currents recorded at potentials close to the open circuit value in order to avoid Faradaic processes. In such a case, the charging current, I_c, is equal to the product of the double layer electrochemical capacitance (C_{DL}) and the scan rate:

$$I_c = \nu C_{DL} \qquad eqn.1$$

To perform an accurate evaluation, C_{DL} was calculated as the slope of the line obtained by plotting I_c vs the scan rate ν. The ECSA value is obtained by dividing C_{DL} by the specific capacitance of the sample (C_s), as reported by McCrory for 1 M NaOH (0.040 mF cm^{-2}).

$$ECSA = \frac{C_{DL}}{C_S} \qquad eqn.2$$

2.3.2 Determination of the catalytic rate constant between glucose and Ni(III) centers

The rate constant for the chemical reaction between glucose and the Ni (III) sites was estimated by chronoamperometry, according to equation 3[16,45,46]:

$$\frac{I_{cat}}{I_L} = \gamma^{0.5}\left[\pi^{0.5} erf(\gamma^{0.5}) + \frac{e^{-\gamma}}{\gamma^{0.5}}\right] \qquad eqn.3$$

where I_{cat} is the catalytic current recorded at the Ni/Al LDH modified electrodes in the presence of glucose, I_L is the limiting current recorded in the same conditions in the absence of glucose and γ is defined as:

$$\gamma = k_{cat} c_o t \qquad eqn.4$$

where k is the reaction kinetic constant, t is the time and c_0 is the glucose concentration.

In the case where γ exceeds 1.5, the second factor of eqn. 3 is almost equal to $\pi^{0.5}$ and the equation can be reduced to:

$$\frac{I_{cat}}{I_L} = \gamma^{0.5}\pi^{0.5} = \pi^{0.5}(k_{cat} c_0 t)^{0.5} \qquad eqn.5$$

The resulting slope of the I_{cat}/I_L versus $c_0^{0.5}$ $t^{0.5}$ plot is equal to $k_{cat}^{0.5}$ $\pi^{0.5}$. For our data the I_{cat}/I_L versus $c_0^{0.5}$ $t^{0.5}$ plot is linear and this indicates a good adherence to the proposed model.

3. RESULTS AND DISCUSSION

3.1 Carbon nanomaterial configuration

The GC electrodes modified with the carbon nanomaterials in different configurations were thoroughly characterized by electrochemical techniques, scanning electron microscopy, UV-Vis and infrared spectroscopies and these results have been reported in our previous publication[43]. The partially restored features of graphene were clearly shown by spectroscopic investigation and by the measurements of surface sheet resistance. Moreover, the electrochemical performances of the CMEs

were investigated for the oxidation of dopamine and catechol. Sharma et al.[43] highlighted that graphene and MWCNTs exhibit a synergistic effect when they are used together as electrode modifiers. The graphene remarkably increases the electrochemically active area of the system, but the π-π stacking of the sheets hinders the diffusion of bulky molecules into the graphene layers. When MWCNTs are present, they are interposed between the graphene sheets leading to an increase of the interlayer distance and, consequently, of the surface accessibility. All the CMEs were used to perform the electrosynthesis of Ni/Al LDH in order to obtain the composite materials.

3.2 Electrosynthesis of Ni/Al LDH

The electrosynthesis of LDH is usually performed by applying a cathodic potential to the working electrodes while they are immersed in a solution containing the nitrate salts of the divalent and trivalent metals. KNO_3 can be added to the electrolyte bath to boost the nitrate reduction reaction. The negative polarization induces the reduction of nitrates and water according to reactions (1-7) in Figure 1 B[31].

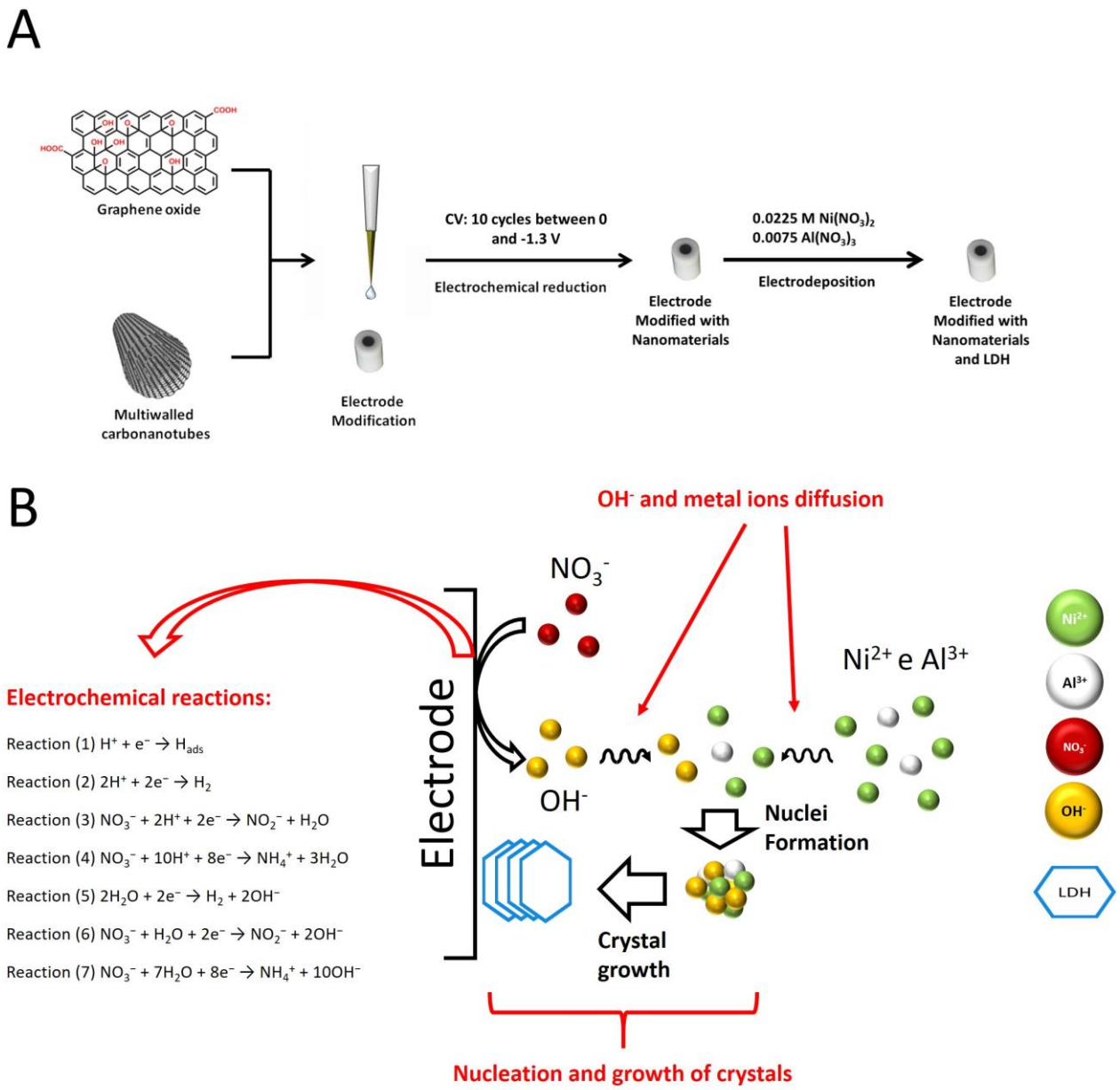

Figure 1. A) Sketch of the electrode preparation. After depositing the nanomaterials on the GC surface by drop casting, an electrochemical reduction is performed to convert the GO to G. Finally, the LDH film is deposited by applying a cathodic potential to the GC electrode. B) Sketch of the main steps involved in the electrosynthesis. The water and nitrate reductions induce a pH increase close to the electrode surface that leads to the LDH precipitation. The hydroxyl ions diffuse from the electrode surface while the Al^{3+} and Ni^{2+} diffuse from the solution bulk. The red arrows and labels highlight the critical points of LDH electrodeposition.

The OH^- production and H^+ depletion induce a pH change from a weakly acidic to a basic solution that causes LDH precipitation on the electrode surface. Although this kind of procedure has been widely used, some weak points can be identified by a study of the literature:

1) *Kinetics of electrochemical OH^- generation.* NO_3^- reduction is usually preferred as the OH^- source because H_2 evolution generates bubbles on the electrode surface that damage the LDH film. Nitrate reduction is a very complex multistep process under a strong kinetic control [47]. The rate of the overall electrochemical reaction depends on the activity of the surface. For example, the activity of Pt can be varied by electrochemical treatment and it highly affects the nature of the electrodeposited LDH films [34].
2) *LDH precipitation*. LDH precipitation involves both the nucleation and growth of crystals, as typical of all the solubility equilibria. Therefore, the rate of the process is controlled by the oversaturation degree of the solution and by the presence of defects on the electrode surface that can act as nucleation centers. Furthermore, the Ni/Al LDH precipitation can follow two different pathways depending on the rate of pH increase [31,48,49]. If the pH slowly increases, $Al(OH)_3$ precipitation takes place first, and, when all the Al^{3+} has been completely consumed, the bivalent cations can be inserted into the amorphous structure of $Al(OH)_3$ to form the layered structure. However, direct precipitation can occur when a quick pH variation occurs.
3) *Reagent diffusion.* LDH precipitation involves three reagents: Me(II), Me(III) and OH^-. The cations diffuse from the solution bulk to the electrode surface, while the hydroxide ions are generated next to the electrode surface and diffuse toward the solution. LDH precipitation should take place on the electrode and it occurs when the OH^- production exactly equalizes the OH^- removal by LDH precipitation[50]. If the OH^- production is slow enough that its concentration is less than the one which can be consumed by Al^{3+}, only $Al(OH)_3$ formation occurs. The reason is that $Al(OH)_3$ precipitates at a pH lower than LDH and Al^{3+} is continuously renewed by diffusion from the solution bulk. On the other hand, when the OH^- production is too fast, OH^- ions diffuse toward the bulk of the solution leading to LDH precipitation also far from the electrode surface. Furthermore, the concentration profiles that are generated close to the electrode surface can lead to a variation of the molar ratio of Me(II)

and Me(III) as a function of the distance from the conductive material, when long potential pulses are applied.

Considering all of these factors, small variations of the electrode surface can significantly affect the LDH deposition, because they modify both the electrochemical activity and the surface density of defects that can act as nucleation sites. In fact, the carbon nanomaterials boost the rate of nitrate reduction as clearly shown in Fig. S1, though the LDH precipitation plays a key role in the overall electrochemical process. The current observed in the presence of Ni^{++} and Al^{+++} ions is significantly higher than the one recorded in KNO_3 solution due to the removal of OH^- following precipitation (Fig. S2). It is worth considering that each electrode undergoes at least one drop casting deposition and an electrochemical reduction to convert GO to ERGO. Therefore, a very robust procedure is necessary to obtain reproducible results during the LDH electrosynthesis.

In order to find the best electrodeposition procedure, we tested three approaches:

1) *Potentiostatic deposition*. The potentiostatic electrodeposition, which is the most commonly used in the literature, is carried out by applying a constant potential to the working electrode (usually between -1.1 and -0.9, vs SCE). Therefore, it is possible to control the thermodynamics of the system and, secondly, the kinetics through the overpotential. Consequently, the applied potential rules the processes that can or cannot occur at the electrode. A process that should be avoided is water reduction, because hydrogen evolution can damage the LDH film. On the other hand, the use of this approach does not ensure a fine control of the rate of OH^- production.
2) *Galvanostatic deposition*. In galvanostatic deposition a constant current flows between the working and the counter electrode. In this way the rate of overall electrochemical processes is forced by the potentiostat and, consequently, the rate of OH^- production should be finely controlled. On the other hand, the applied potential must be varied to guarantee the instrument operation and, thus, it is more difficult to control the side processes.

3) *Potentiodynamic electrodeposition*. In a potentiodynamic approach, the deposition is stimulated by performing a cyclic voltammetry on the cathodic side from 0 to -1.35 V. The most anodic potential is fixed far from the onset potential of the deposition in order to have enough time to restore the cation concentration close to the electrode surface by diffusion. Moreover, the value of the most cathodic potential can be fixed in order to avoid the occurrence of side reactions.

The three different approaches were carried out using the electrode modified with graphene as benchmark and the reproducibility of the procedures was tested by evaluating the peak currents associated with the redox signal of Ni centers according to reaction 1.

Reaction (1) Ni(II)-LDH + OH^- ⇄ Ni(III)-LDH + e^-

Fig. 2 A-C shows three CVs relevant to the potentiostatic, galvanostatic and potentiodynamic procedures already optimized to obtain the best results in terms of reproducibility of the electrochemical signal. The potentiostatic deposition exhibits the worst robustness on ERGO/GC probably because it does not allow a fine control of the OH^- production and, thus, of the amount of precipitated LDH. On the other hand, when the synthesis is performed by a galvanostatic or potentiodynamic procedure, the results display good reproducibility with a relative standard deviation of the peak current equal to 10 and 7 %, respectively. The potentiodynamic synthesis was chosen for subsequent experiments involving the five configuration of carbon nanomaterials because it shows the best reproducibility. Furthermore, the results obtained were compared with those relevant to the potentiostatic synthesis due its wide use (Fig. 2 D and E). It is worth mentioning that the conditions chosen for the potentiodynamic deposition led to a LDH film with higher peak currents than the potentiostatic one. The key point is that when the films are obtained by potentiostatic deposition, the associated percentage error is very high and is often comparable with the peak current. Since the amount of electrodeposited material is very low and can be exploited for only one characterization, we chose to thoroughly study the potentiodynamic deposition because the uncertainty of the

potentiostatic procedure could lead to misleading results. Such results highlights that the drop casting procedure leads to GCEs modified with the carbon nanomaterials in a simple and rapid way and allows to obtain a reproducible LDH film by electrosynthesis if the optimized potentiodynamic approach is employed.

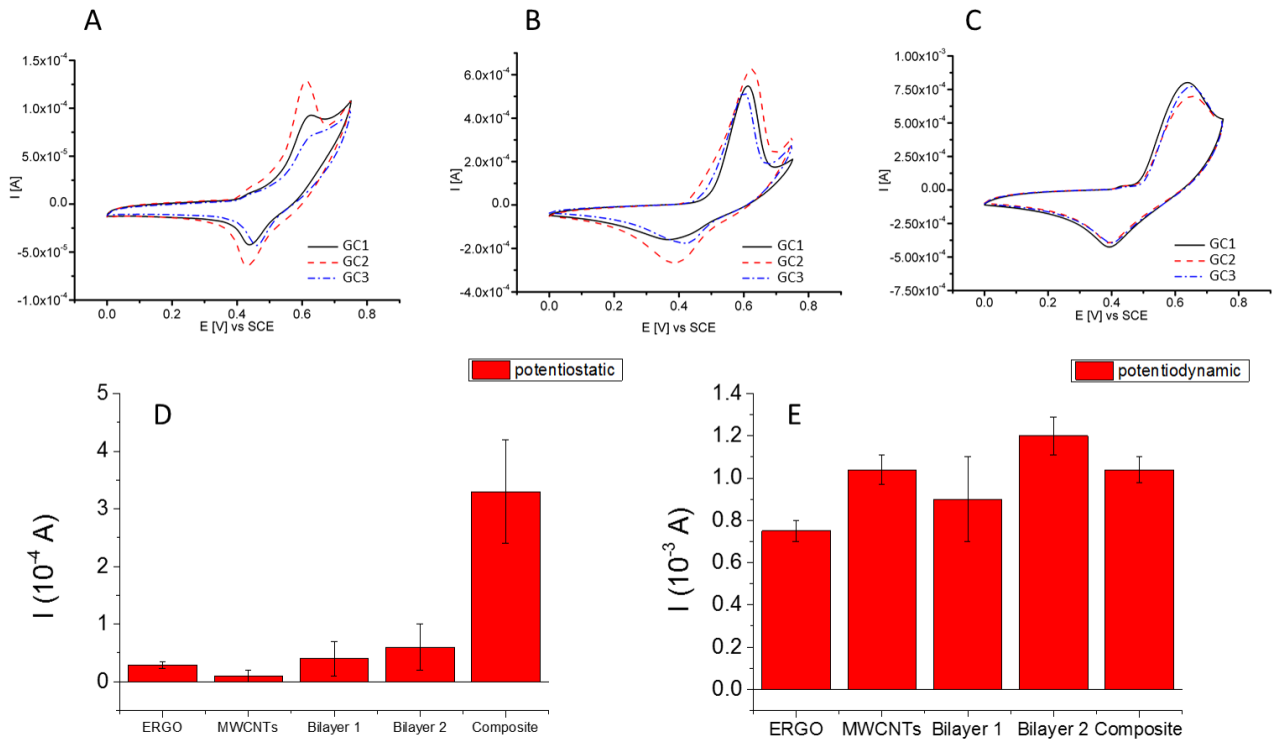

Figure 2. CVs (scan rate = 0.050 V s^{-1}) recorded in 0.1 M NaOH for three LDH/ERGO/GC electrodes resulting from potentiostatic (A), galvanostatic (B) and potentiodynamic (C) electrodepositions. Peak current values (average ± standard deviation obtained from 3 different electrodes) relative to electrodes obtained for the potentiostatic (D) and potentiodynamic (E) electrodepositions carried out on GC modified with the five nanomaterial configurations.

3.3 Structural characterization

The thin films obtained by potentiodynamic synthesis were characterized by powder X-Ray diffraction (PXRD) to confirm the formation of a LDH structure. Six cycles of voltammetry were performed during the synthesis to obtain a enough LDH to record the diffractograms. After drying at

60 °C for 45 min, the LDH coatings were gently removed from the GC electrodes. Fig. 3 shows the diffractograms of LDHs electrodeposited on a bare GC and on GC electrodes modified by the carbon nanomaterials in the five configurations. All the films exhibit a pattern that is ascribable to a LDH. The peaks at about 10°, 20° and 34.8° are ascribable to the reflections of the crystallographic planes labelled with Miller indexes 003, 006 and 012. All reflections are broad and weak suggesting that electrosynthesized LDHs exhibit a low crystallinity. Finally, the distances between brucite layers were calculated from the 003 reflection and range between 0.84 and 0.89 nm, in agreement with the intercalation of nitrate anions in the interlayer region.

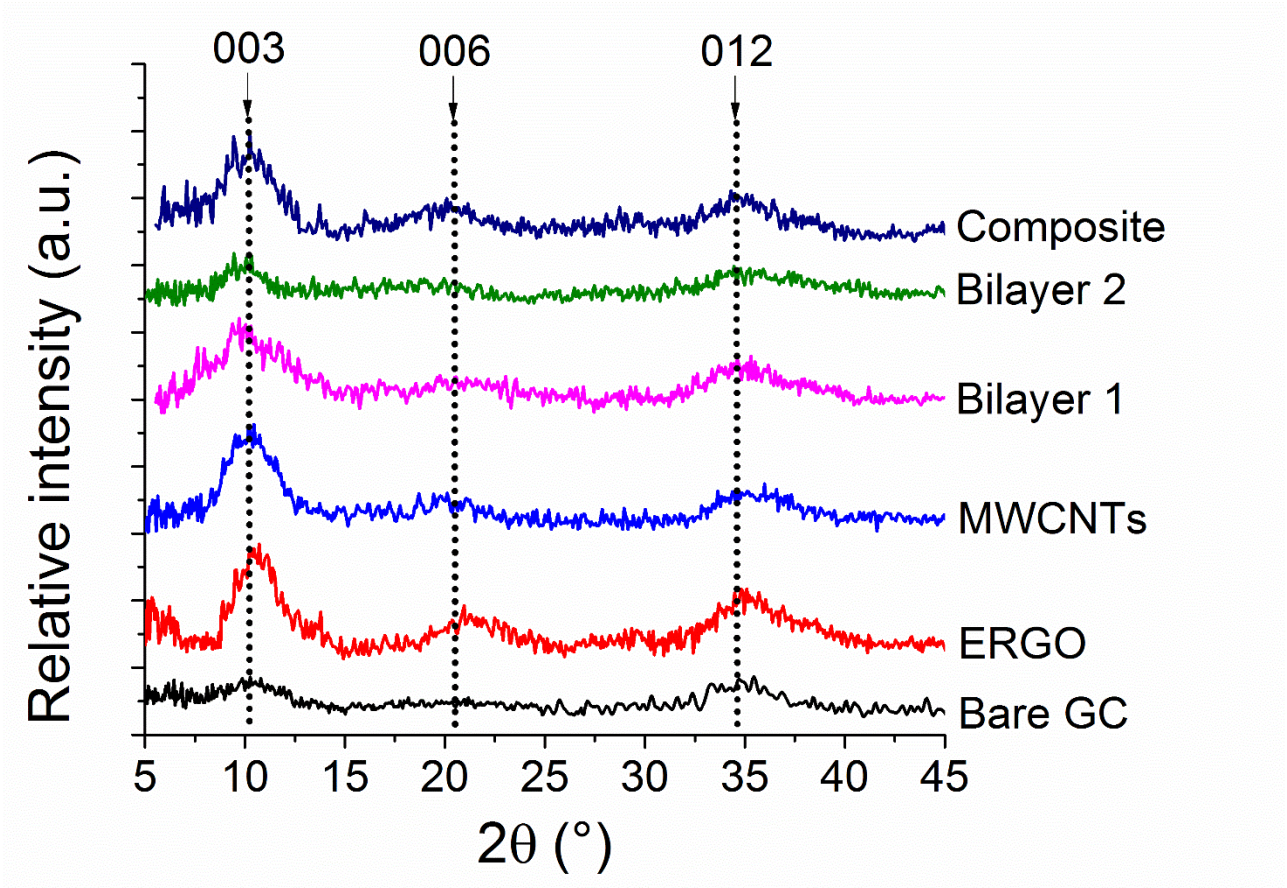

Figure 3. PXRD patterns recorded for LDH synthesized by the potentiodynamic approach.

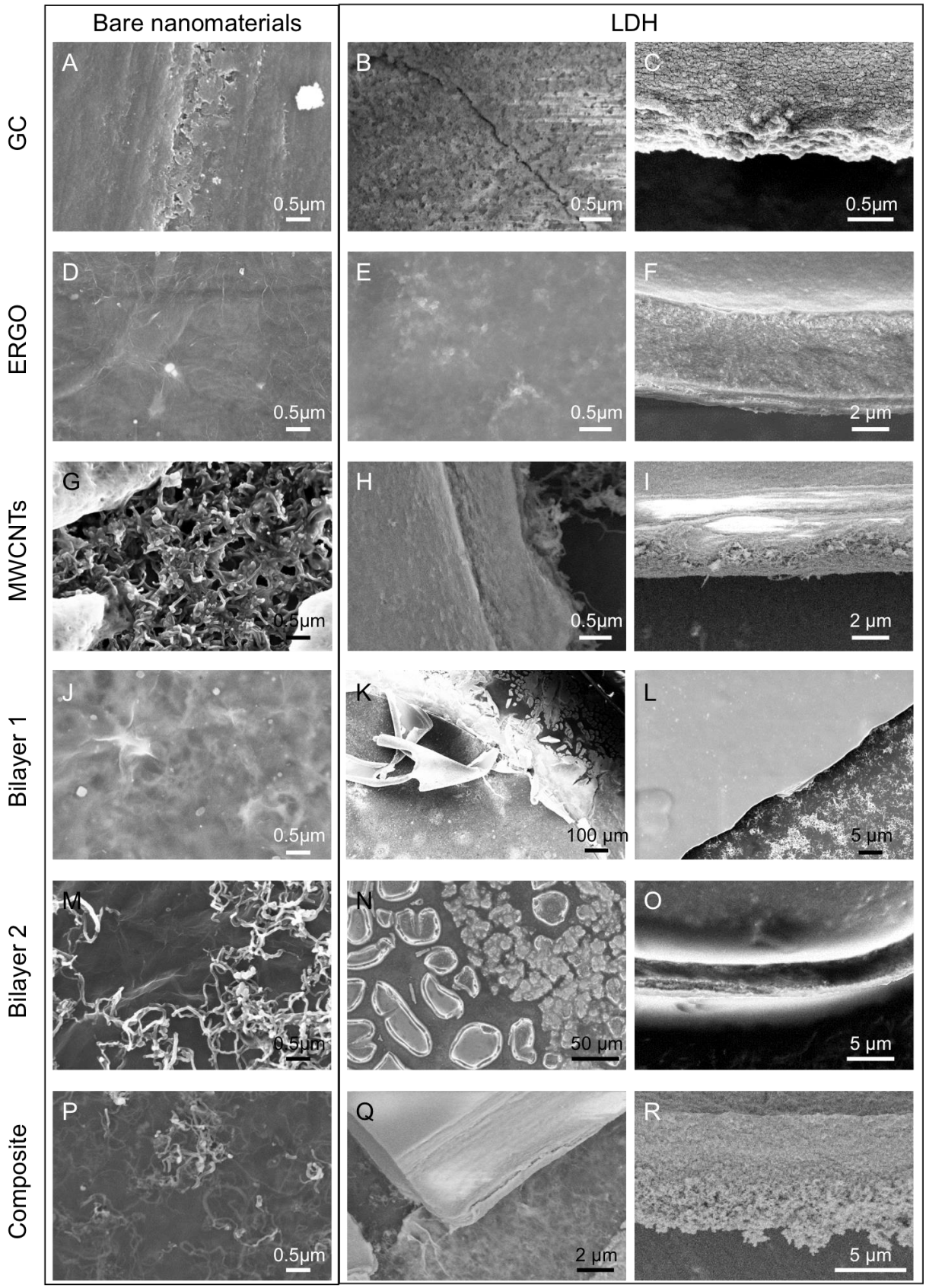

Figure 4. SEM images for bare GC (A), ERGO/GC (D), MWCNTs/GC (G), Bilayer1/GC (J), Bilayer2/GC (M), Composite/GC (P), LDH/GC (B) and (C), LDH/ERGO/GC (E) and (F), LDH/MWCNTs/GC (H) and (I), LDH/Bilayer1/GC (K) and (L), LDH/Bilayer2/GC (N) and (O) and LDH/Composite/GC (Q) and (R).

3.4 Morphological characterization

The morphology of the LDH films was investigated by field emission Scanning Electron Microscopy (SEM). Fig. 4 shows the images of the bare GC and GC modified with the nanomaterials before and after the electrochemical deposition. The surface of the bare GC is flat with some scratches due to the mechanical polishing (Fig. 4 A). ERGO/GC displays a wrinkled texture, which is due to the structural rearrangements occurring after the removal of the hydroxyl and epoxide functionalities from the GO and the consequent recovery of the conjugated systems (Fig. 4 D). In MWCNTs/GC (Fig. 4 G), the nanotubes appear as cylindrical nanostructures, with a diameter between 30 and 60 nm, which are entangled with each other on the GC surface. In the Bilayer 1 configuration (Fig. 4 J), the ERGO is on the top of the electrode surface and, consequently, the surface appears quite smooth. The MWCNTs are still visible, but they are less clear because they are underneath the ERGO layer. The Bilayer2/GC is composed of MWCNTs on an ERGO layer and both layers are clearly visible in Fig. 4 M. The Composite/GC exhibits a uniform and smooth layer with embedded nanotubes (Fig. 4 P). The graphene sheets are not readily apparent, but their presence is suggested by the appearance of MWCNTs with different contrast in the same image. The nanotubes which are at a greater depth in the composite appear less clear, while the ones that are closest to the surface appear brighter and more sharply defined (Fig 4 P).

The LDH/GC shows a homogeneous and compact layer with a textured surface due to the very small LDH crystallites, as shown in Fig. 4 B and C, where the surface and the cross-section are shown respectively. On the other hand, the LDH films appear smooth when they were synthesized on the electrodes modified with nanomaterials in the five configurations (Fig. 4 E-Q). The LDH morphology changes for the electrosynthesis carried out on the different modified electrodes, because carbon nanomaterials affect both the rate of OH^- production and the LDH nucleation. In fact, the cross-sectional images in Fig. 4 F, I, O, R show the electrodes covered by a very thin film that could be constituted of amorphous hydroxides that did not have time to be converted into the lamellar structure.

Under this upper layer the Ni/Al LDHs films are usually rough, and the LDH layers are penetrated by MWCNTS, especially when the nanotubes are on the top of the GC or ERGO rather than below (Fig. 4 I and O, for LDH/MWCNTs/GC and LDH/Bilayer2/GC respectively, even if the morphology of the latter is difficult to see because of charging effects). The interpenetration of different layers could help the charge transport phenomena in the film. The cross section of LDH/ERGO/GC shows the presence of an ERGO layer under the LDH and the two materials exhibit a poor interpenetration. Finally, Fig. 4 R displays that LDH/Composite/GC displays a uniform layer without a separation between LDH and carbon nanomaterials. It is worth noting that the films obtained using the bilayer configurations exhibit a scarce adhesion especially on Bilayer 1, and after drying, the film can detach from the electrode surface in some points, as shown in Fig. 4 K, - delamination of the film is reported - and in N – partial coverage due to dewetting effects. Finally, the elemental compositions of the LDH films were investigated by EDX analysis (Tab. S1) that showed a molar ratio Ni/Al that is compatible with LDH structure, even if always lower the value of the electrolytic solution.

3.5 Electrochemical Characterization

The GC electrodes modified with the LDHs and nanomaterials were electrochemically characterized by CV and electrochemical impedance spectroscopy.

All CVs show a clearly visible Faradaic process that takes place at a formal potential of about 0.54 V that is characteristic of Ni/al LDH[51,52]. Accordingly, our previous work[18] has investigated by XPS the oxidation state of LDH before and after the occurrence of the oxidation peak. The pristine LDH shows Ni centers that are almost in + 2 oxidation state, while after the oxidation peak we observed the formation Ni(III) centers highlighting that the redox wave is associated to Ni(II)/Ni(III) couple. The redox potentials display small shifts for the different configurations of nanomaterials. If on the one hand, the peak potentials are independent of the underlying carbon nanomaterial configuration, on the other hand the peak current values are strongly dependent. Fig. 5 A highlights that the presence of MWCNTs plays a key role in generating a large amount of electroactive Ni centers. In fact, the

highest Faradaic responses are observed for the configurations with the MWCNTs in the upper part of the carbon nanomaterial layers (LDH/Bilayer2/GC and LDH/MWCNTs/GC) while the lowest currents are recorded for the LDH/ERGO/GC. LDH/Composite/GC and LDH/Bilayer1/GC display peak current values that are between those recorded at LDH/ERGO/GC and LDH/MWCNTs/GC, whereas LDH/GC exhibits the lowest peak current.

Furthermore, the electrochemically active areas, estimated using the approach proposed by McCrory et al.[44], of the electrodes modified with LDHs and nanomaterials strongly depend on the presence of ERGO, as previously reported for GC modified with only carbon nanomaterials. In fact, bare LDH/GC and LDH/MWCNTs/GC exhibit the lowest ESCA, while LDH/ERGO/GC and LDH/Bilayer2/GC display the highest values.

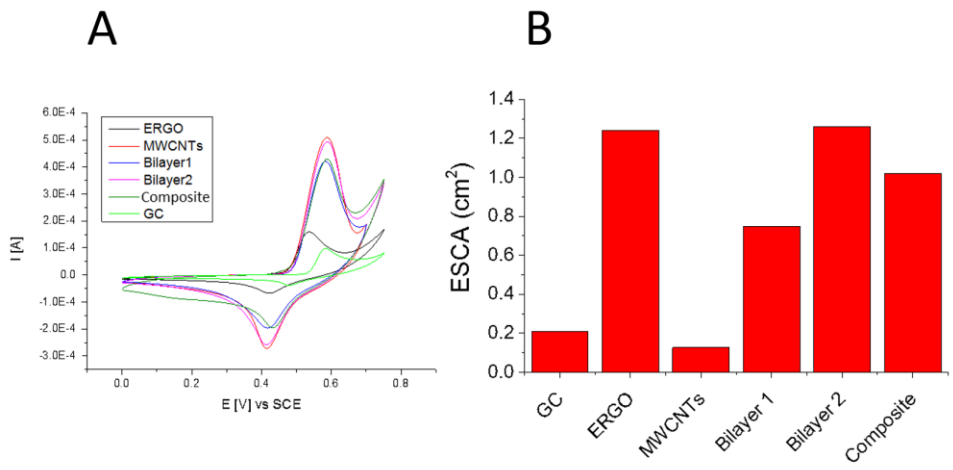

Figure 5. CVs (A) (scan rate = 0.010 V s^{-1}, recorded in 0.1 M NaOH) and relevant ESCA values (B) obtained for all the LDH potentiodynamic electrodepositions on bare and modified GCs.

Electrochemical Impedance Spectra (EIS) tests were performed to investigate the charge transfer processes taking place at LDH/GC and LDHs obtained on GC electrodes modified with the different carbon nanomaterials (Fig. 6 A). The data were plotted in the form of Nyquist plots and the spectra were simulated using the equivalent circuit shown in Fig. 6 B.

R_{el}, in the high frequency region, is the resistance associated with the electrolytic solution; R_{ct1} and C_1, in the middle frequency region, are respectively a resistance and a capacitance related to the interface-modified electrode-solution. The parallel element $R_{ct2\text{-}Cc}$ LDH accounts for the arc lying in the low frequency region and it is the most important one in the characterization of the electrode coating because it describes the charge transfer processes between the carbon nanomaterials and the LDH. Moreover, a Constant Phase Element was added in the equivalent circuit to simulate the diffusion processes occurring inside the LDHs because of the inter-penetration of the hydroxide with carbon nanomaterials that generates inhomogeneity at these interfaces.

Table 1 reports the values of the circuital elements for each modified electrode. From the data we can see that, as expected, R_{el}, R_{ct1} and C_1 are quite independent of the type of carbon material used, while R_{ct2} strongly depends on the composite material, since the LDH-carbon material interfaces affect the rate of charge transfer. When the LDH is deposited on bare GC, the highest resistance (28 x10^2 Ω) is observed, highlighting that the nanomaterials lead to a significant improvement in the charge transfer processes involving the Ni/Al LDH. Among carbon nanomaterials, the presence of graphene sheets boosts the charge transfer processes because all composite materials (LDH/Bilayer1/GC, LDH/Bilayer2/GC and LDH/Composite/GC) and LDH/ERGO/GC exhibit significantly lower resistances than that associated with LDH/MWCNTs/GC. These phenomena can be explained considering that the graphene exhibits high ESCA values that lead to an increased contact area with LDH surface, generating an improvement in the charge transfer processes.

The electrochemical characterizations highlight the synergistic effect stemming from the interaction of carbon nanomaterials with LDH. The redox behavior of CMEs is surely ruled by the Ni(III)/Ni(II) couple of LDH, which is the material that exhibits the most interesting features for the fabrication of sensors, supercapacitors and fuel cells. The presence of carbon nanomaterials significantly improves the performance of the electrode modifier. EIS clearly shows that MWCNTs and ERGO in their different configurations investigated boost the charge transfer processes between GC and Ni centers.

This is a key point to produce electrochemical interfaces that can ensure high efficiencies through the sustenance of high current flow rates generated by fast and/or intense redox processes. On the one hand, the CV analysis highlights that the presence of MWCNTs allows a film with a high number of redox active Ni centers to be obtained. On the other hand, ERGO ensures high ESCA values that, consequently, increase the roughness of the electrode modifier. This feature is important for the design of electrochemical devices, because high roughness values allow an efficient mass transport from the solution bulk to the redox active material with beneficial effects for the above-mentioned applications. The electrochemical characterization highlights that the composite materials proposed here exhibit an improvement in electrochemical performance that is analogous to that observed for the LDH/G and LDH/CNT composite materials obtained by bulk synthesis protocols [13,14,22–24,27,28]. In fact, MWCNTs and ERGO help the charge transport inside the LDH that exhibits a relatively low electrical conductivity. As previously reported by Guo et al.[53], graphene sheets act as bridging sites between the electrode surface and the hydroxide and the same effect was observed for carbon nanotubes. Moreover, it was reported that carbon nanomaterial can improve the LDH adhesion on GC by forming a "nanoglue"[38]. Obviously, this strict contact also enhances the charge transfer process at the electrode surface.

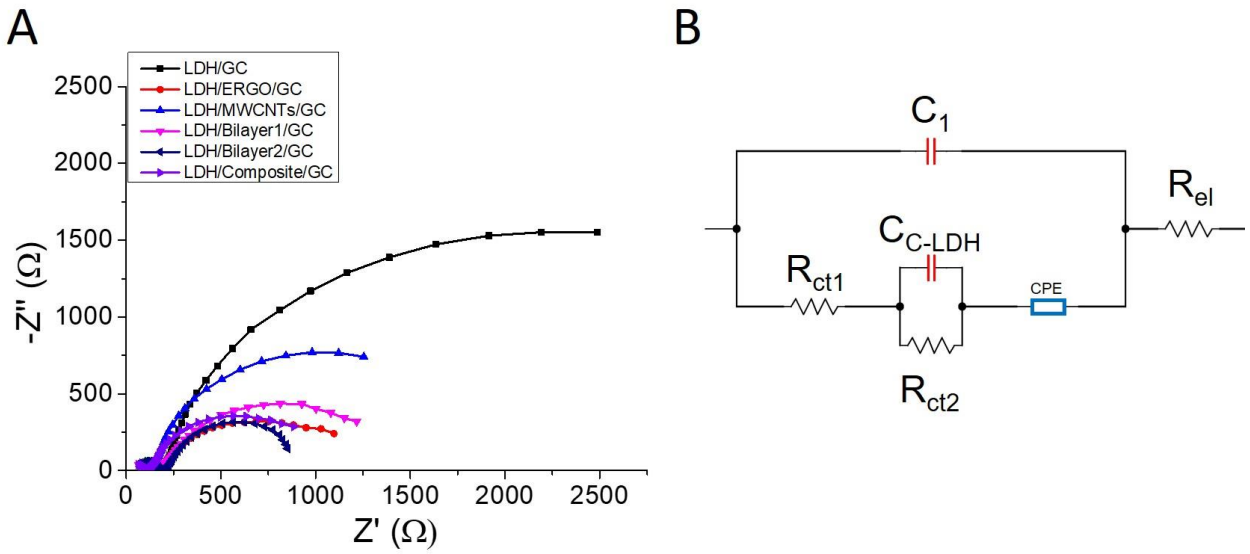

Figure 6. A) Nyquist plot recorded in 0.1 M NaOH for LDH/GC and LDHs electrosynthesized on GC electrodes modified with the different configurations of carbon nanomaterials. B) Equivalent circuit used for the data interpolation.

Table 1. Parameters obtained by fitting the Nyquist plot in Figure 6.

	LDH/GC	LDH/ERGO/GC	LDH/MWCNTs/GC	LDH/Bilayer1/GC	LDH/Bilayer2/GC	LDH/Composite/GC
C_1 (F)	1.7×10^{-8}	1.5×10^{-8}	2.7×10^{-8}	2.2×10^{-8}	1.7×10^{-8}	2.8×10^{-8}
$C_{C\text{-}LDH}$ (F)	2.8×10^{-3}	5.8×10^{-3}	6.5×10^{-3}	5.8×10^{-3}	5.1×10^{-3}	7.4×10^{-3}
R_{ct1} (Ω)	76	110	85	67	116	74
R_{ct2} (Ω)	28×10^{2}	5.8×10^{2}	13×10^{2}	7.4×10^{2}	5.4×10^{2}	6.1×10^{2}
R_{el} (Ω)	32	36	41	29	53	36
Q ($\Omega\ s^{-Qn}$)	6.3×10^{-3}	7.6×10^{-3}	14×10^{-3}	5.4×10^{-3}	11×10^{-3}	14×10^{-3}
Q_n	0.17	0.34	0.44	0.22	0.24	0.36

3.6 Glucose sensing

All the modified LDH/GC electrodes were exploited as electrochemical sensors for glucose detection and the results were compared with those recorded for LDH/GC. The Ni/Al LDH promotes the glucose electrocatalytic oxidation in basic medium according to the following reaction scheme [52]:

Reaction (1) $\quad Ni(II)/Al\ LDH \rightarrow Ni(III)/Al\ LDH + e^-$

Reaction (2) $\quad n\ Ni(III)/Al\ LDH + Glucose \rightarrow n\ Ni(II)/Al\ LDH + Oxidized\ Glucose$

Firstly, Ni(II) center are oxidized to Ni(III) and than Ni(II)/Al are re-obtained by reaction 2, i.e., by the electrocatalytic process, thus generating higher currents than those recorded without glucose. The sensor behavior was investigated by chronoamperometry (E = + 0.6 V) under magnetic stirring while the glucose concentration was increased (Fig. 7 A). Each glucose addition generated a variation of current that was linearly related to concentration (inset Fig. 7 A). The sensor performances were evaluated in terms of sensitivity. The sensitivity is expressed as the slope of the calibration plots and is reported with the relative error calculated for three different electrodes (Fig. 7 B). LDH/MWCNTs/GC, LDH/Bilayer2/GC and LDH/Composite/GC show the highest sensitivities. Since these values are not statistically different from each other, we can hypothesize that the rate determining step in the overall electrochemical process is independent of the electrode modifier because the rate of charge transfer overcomes that of glucose mass transport from the solution bulk.

Therefore, the only process that can control the current is analyte diffusion to the electrode surface. Among the other modified electrodes, the LDH/GC electrode displays the lowest sensitivity suggesting that the carbon nanomaterials play a key role.

To better understand the transduction process, the catalytic constant (k_{cat}) of glucose oxidation (constant of reaction 2) was estimated according to recent literature [16,45,46]. All the k_{cat} values are close to each other and range from 1.8 to 8.0 M^{-1} s^{-1}. These results highlight that the presence of carbon nanomaterials does not improve the chemical reactivity of the LDH Ni centers. Therefore, the higher sensitivities recorded when LDH is deposited on a GC surface previously modified with carbon nanomaterials are due to the boosted charge transfer between the GC electrode and Ni centers. MWCNTs and ERGO help the transfer of electrons from the Ni centers to the GC surface with an increase of the current observed during the glucose detection. Obviously, this generates an improvement of sensor performance that is demonstrated by high sensitivities values.

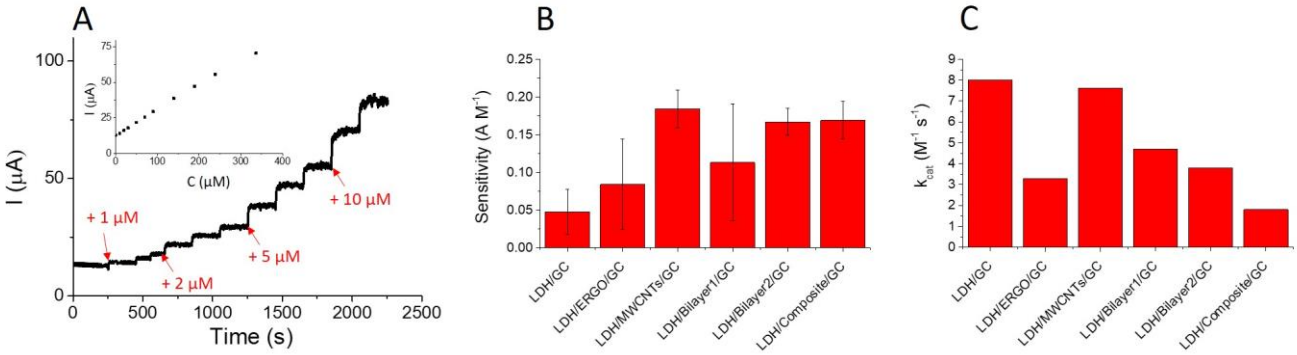

Figure 7. A) I vs time plot obtained for LDH/composite/GC applying + 0.6 V in 0.1 M NaOH under magnetic stirring while the glucose concentration was increased by progressive addition of a concentrated solution (Inset: calibration plot obtained from the current values of figure 7 A). B) Sensitivities (average ± standard deviation obtained for 3 different electrodes) to glucose relevant to all electrodes modified with Ni/Al LDH. C) K_{cat} for glucose electrooxidation evaluated for the LDH films generated on bare GC and GC electrodes modified with the nanomaterials in the 5 configurations.

The response stability was studied by recording two calibration curves with the same electrode and it was expressed by the percentage decrement of calibration slope (Table S2). LDH/GC,

LDH/ERGO/GC, LDH/Bilayer1/GC and LDH/Composite/GC show a poor stability, with a decrease of the slope ranging from 28 to 74 %. The loss of electrochemical activity can be explained by considering that the glucose oxidation is a complex redox process and some reaction intermediates can be adsorbed on the electrode modifier and, consequently, the electrocatalytic processes slow down. On the other hand, LDH/MWCNT/GC and LDH/Bilayer2/GC display a good stability highlighting that a key factor for the application as sensors for glucose is the presence of MWCNTs at carbon nanomaterials/LDH interface. In addition, LDH/MWCNT/GC and LDH/Bilayer2/GC keep a stability of the response for one week if the devices are stored in 0.1 M NaOH solution.

Table 2 compares the performances of the chemically modified electrodes reported in this work with others based on layered double hydroxide, already described in literature. When the comparison is limited to the devices prepared by electrochemical deposition, it can be noticed that LOD values are lower if the approach is potentiodynamic rather than potentiostatic, as demonstrated by the values reported for Ni/Al LDH/GC. Furthermore, the presence of carbon nanomaterials allows for an additional improvement of the LOD values in respect with the NiAl LDH/GC. The sensitivities of NiAl LDH/MWCNTs/GC, NiAl LDH/Bilayer2/GC and NiAl LDH/Composite/GC are very close to the ones recorded for other electrodes prepared by electrochemical deposition, thus confirming that the response is kinetically limited by the mass transport at electrode surface.

When the comparison is extended to all devices, the sensitivities of NiAl LDH/MWCNTs/GC, NiAl LDH/Bilayer2/GC and NiAl LDH/Composite/GC are usually higher than those observed for the electrodes modified with LDHs deriving from a chemical synthesis, except for the case of NiMn-LDH/GO. On the contrary, the LOD values are better for the electrodes modified with chemical synthesized LDHs.

Table 2. Comparison with other reported LDH modified electrodes

	Sythesis	Sensitivity (A M^{-1} cm^{-2})	LOD (μM)	Durability	ref
NiAl LDH/GC	Electrochemical potentiodynamic	0.7	2		This work
NiAl LDH/ERGO/GC	Electrochemical potentiodynamic	1.2	1		This work
NiAl LDH/MWCNT/GC	Electrochemical potentiodynamic	2.6	0.8	One week	This work
NiAl LDH/Bilayer1/GC	Electrochemical potentiodynamic	1.6	3		This work
NiAl LDH/Bilayer2/GC	Electrochemical potentiodynamic	2.4	0.9	One week	This work
NiAl LDH/Composite/GC	Electrochemical potentiodynamic	2.4	0.6		This work
CoAl LDH/Pt	Electrochemical potentiostatic	2.61	9	One month	[54]
NiAl LDH/Pt	Electrochemical potentiostatic	2.64	10	12 days	[52]
MnO_2/Co_3O_4	Chemical synthesis	0.127	0.03	One week	[55]
NiAl LDH/graphene-CNT/GC	Chemical synthesis	1.989	1	30 days	[56]
CuAl-LDHs/GCE	Chemical synthesis	0.112	0.02	15 days	[57]
NiMn-LDH/GO	Chemical synthesis	0.839	1.2	-	[58]
NiCo LDH/Carbon cloth	Chemical synthesis	5.12	0.12	1 month	[59]

4. CONCLUSION

LDHs can be combined with MWCNTs and graphene at nanoscale level to produce new materials for electrochemical applications with enhanced performance. Although several synthesis protocols have been proposed, the electrochemical route remain still less explored. For the first time, we propose a synthetic route that allows for the electrochemical synthesis of an LDH on GC electrodes previously modified with MWCNTs and/or ERGO combined in five different configurations. To this aim, different approaches have been investigated and the potentiodynamic procedure based on CV ensures the best performance in terms of reproducibility of the electrochemical response.

The presence of carbon nanomaterials significantly improves the electrochemical performance of GC modified with LDH by boosting the rate of charge transfer between the electrode and the Ni centers as demonstrated by CV and EIS investigations. In fact, the LDH deposited on GC exhibits a charge transfer resistance that is significantly higher than the one recorded for the LDH in close contact with the nanomaterials. In addition, the presence of graphene significantly increases the electrochemically active area of the LDH modified electrodes. All these features are very promising for the design of electrochemical interfaces because they allow the electrode modifier to be efficiently exploited by minimizing the resistance to the mass transport from the solution and the charge transfer with the electrode surface. Finally, the modified electrodes were employed as glucose sensors demonstrating that carbon nanomaterials play a key role in the improvement of performance. In fact, the electrodes show limits of detection that are one order of magnitude lower than those reported in literature for other chemically modified electrodes based on electrodeposited LDHs. Moreover, also the sensitivities are very high when the performances are compared with other sensors based on LDHs. These interfaces will be studied in a next future for other electrochemical applications such as supercapacitors and electrocatalysis on the basis of their superior performance in terms of charge transfer rate.

5. ASSOCIATED CONTENT

Supporting information.

Electrochemical reduction of NO_3^- on carbon nanomaterials, effect of metal cations on nitrate reduction, EDS analysis, stability of sensors

6. AUTHOR INFORMATION

Corresponding Author

e-mail: domenica.tonelli@unibo.it

ORCID:

Domenica Tonelli: 0000-0002-2844-9817

Isacco Gualandi: 0000-0002-6823-7501

Meganne Christian: 0000-0001-6123-2014

Vittorio Morandi: 0000-0002-8533-1540

Erika Scavetta: 0000-0001-7298-0528

Elisa Musella: 0000-0003-3465-6668

Marco Giorgetti: 0000-0001-7967-8364

Author contribution:

LM and YV carried out electrochemical experiments. IG and DT planned and designed the experiments. ES designed EIS experiments. MC and VM carried out morphological characterization. IG wrote the article. DT supervised the research project. All the authors discussed the results and revised the text.

Funding source:

The European Union's Horizon 2020 research and innovation programme under Grant Agreement no. 785219 Graphene Flagship

7. ACKNOWLEGEMENTS

The authors thanks dott. Gazzano for performing the PXRD analysis. The European Union's Horizon 2020 research and innovation programme under Grant Agreement no. 785219 Graphene Flagship is gratefully acknowledged.

8. REFERENCES

(1) Wang, G.; Z; Hang, L.; Zhang, J. A Review of Electrode Materials for Electrochemical Supercapacitors. *Chem. Soc. Rev.* **2012**, *41*, 797–828. https://doi.org/10.1039/c1cs15060j.

(2) Bhojane, P.; Sen, S.; Shirage, P. M. Enhanced Electrochemical Performance of Mesoporous $NiCo_2O_4$ as an Excellent Supercapacitive Alternative Energy Storage Material. *Appl. Surf. Sci.* **2016**, *377*, 376–385. https://doi.org/10.1016/j.apsusc.2016.03.167.

(3) Etacheri, V.; Marom, R.; Elazari, R.; Salitra, G.; Aurbach, D. Challenges in the Development of Advanced Li-Ion Batteries : A Review. *Energy Environ. Sci.* **2011**, *4*, 3243–3262. https://doi.org/10.1039/c1ee01598b.

(4) Bhojane, P.; Sinha, L.; Devan, R. S.; Shirage, P. M. Mesoporous Layered Hexagonal Platelets of Co3O4nanoparticles with (111) Facets for Battery Applications: High Performance and Ultra-High Rate Capability. *Nanoscale* **2018**, *10*, 1779–1787. https://doi.org/10.1039/c7nr07879j.

(5) Boghossian, A. A.; Sen, F.; Gibbons, B. M.; Sen, S.; Faltermeier, S. M.; Giraldo, J. P.; Zhang, C. T.; Zhang, J.; Heller, D. A.; Strano, M. S. Application of Nanoparticle Antioxidants to Enable Hyperstable Chloroplasts for Solar Energy Harvesting. *Adv. Energy Mater.* **2013**, *3*, 881–893. https://doi.org/10.2298/JSC150429078T.

(6) Kirubakaran, A.; Jain, S.; Nema, R. K. A Review on Fuel Cell Technologies and Power Electronic Interface. *Renew. Sustain. Energy Rev.* **2009**, *13*, 2430–2440. https://doi.org/10.1016/j.rser.2009.04.004.

(7) Daşdelen, Z.; Yıldız, Y.; Eriş, S.; Şen, F. Enhanced Electrocatalytic Activity and Durability of Pt Nanoparticles Decorated on GO-PVP Hybride Material for Methanol Oxidation Reaction. *Appl. Catal. B Environ.* **2017**, *219*, 511–516. https://doi.org/10.1016/j.apcatb.2017.08.014.

(8) Başkaya, G.; Yıldız, Y.; Savk, A.; Okyay, T. O.; Eriş, S.; Sert, H.; Şen, F. Rapid, Sensitive, and Reusable

Detection of Glucose by Highly Monodisperse Nickel Nanoparticles Decorated Functionalized Multi-Walled Carbon Nanotubes. *Biosens. Bioelectron.* **2017**, *91*, 728–733. https://doi.org/10.1016/j.bios.2017.01.045.

(9) Tonelli, D.; Scavetta, E.; Giorgetti, M. Layered-Double-Hydroxide-Modified Electrodes: Electroanalytical Applications. **2013**, 603–614. https://doi.org/10.1007/s00216-012-6586-2.

(10) Shao, M.; Zhang, R.; Li, Z.; Wei, M.; Evans, D. G.; Duan, X. Layered Double Hydroxides toward Electrochemical Energy Storage and Conversion: Design, Synthesis and Applications. *Chem. Commun.* **2015**, *51*, 15880–15893. https://doi.org/10.1039/c5cc07296d.

(11) Mousty, C. Biosensing Applications of Clay-Modified Electrodes: A Review. *Anal. Bioanal. Chem.* **2010**, *396*, 315–325. https://doi.org/10.1007/s00216-009-3274-y.

(12) Cavani, F.; Trifirò, F.; Vaccari, A. Hydrotalcite-Type Anionic Clays: Preparation, Properties and Applications. *Catal. Today* **1991**, *11*, 173–301. https://doi.org/10.1016/0920-5861(91)80068-K.

(13) Varadwaj, G. B. B.; Nyamori, V. O. Layered Double Hydroxide- and Graphene-Based Hierarchical Nanocomposites: Synthetic Strategies and Promising Applications in Energy Conversion and Conservation. **2016**, *9*, 3598–3621. https://doi.org/10.1007/s12274-016-1250-3.

(14) Wang, H.; Xiang, X.; Li, F. Facile Synthesis and Novel Electrocatalytic Performance of Nanostructured Ni – Al Layered Double Hydroxide/Carbon Nanotube Composites. *J. Mater. Chem.* **2010**, *20*, 3944–3952. https://doi.org/10.1039/b924911g.

(15) Liu, X.; Zhang, Y.; Zhang, X.; Fu, S. Studies on Me/Al-Layered Double Hydroxides (Me = Ni and Co) as Electrode Materials for Electrochemical Capacitors. *Electrochim. Acta* **2004**, *49*, 3137–3141. https://doi.org/10.1016/j.electacta.2004.02.028.

(16) Gualandi, I.; Scavetta, E.; Zappoli, S.; Tonelli, D. Electrocatalytic Oxidation of Salicylic Acid by a Cobalt Hydrotalcite-like Compound Modified Pt Electrode. *Biosens. Bioelectron.* **2011**, *26*, 3200–3206. https://doi.org/10.1016/j.bios.2010.12.026.

(17) Zebda, A.; Tingry, S.; Innocent, C.; Cosnier, S.; Forano, C.; Mousty, C. Hybrid Layered Double Hydroxides-Polypyrrole Composites for Construction of Glucose/O_2 Biofuel Cell. *Electrochim. Acta* **2011**, *56*, 10378–10384. https://doi.org/10.1016/j.electacta.2011.01.101.

(18) Vlamidis, Y.; Fiorilli, S.; Giorgetti, M.; Gualandi, I.; Scavetta, E.; Tonelli, D. Role of Fe in the Oxidation of Methanol Electrocatalyzed by Ni Based Layered Double Hydroxides: X-Ray Spectroscopic and Electrochemical Studies. *RSC Adv.* **2016**, *6*, 110976–110985. https://doi.org/10.1039/C6RA19192D.

(19) Lu, Z.; Xu, W.; Zhu, W.; Yang, Q.; Lei, X.; Liu, J.; Li, Y.; Sun, X.; Duan, X. Three-Dimensional NiFe Layered Double Hydroxide Film for High-Efficiency Oxygen Evolution. *Chem. Commun.* **2014**, *2*, 6479–6482. https://doi.org/10.1039/c4cc01625d.

(20) Vlamidis, Y.; Scavetta, E.; Gazzano, M.; Tonelli, D. Iron vs Aluminum Based Layered Double Hydroxides as Water Splitting Catalysts. *Electrochim. Acta* **2016**, *188*, 653–660. https://doi.org/10.1016/j.electacta.2015.12.059.

(21) Wang, Y.; Chen, Z.; Li, H.; Zhang, J.; Yan, X.; Jiang, K.; den Engelsen, D.; Ni, L.; Xiang, D. The Synthesis and Electrochemical Performance of Core-Shell Structured Ni-Al Layered Double Hydroxide/Carbon Nanotubes Composites. *Electrochim. Acta* **2016**, *222*, 185–193. https://doi.org/10.1016/j.electacta.2016.09.073.

(22) Zhao, J.; Chen, J.; Xu, S.; Shao, M.; Zhang, Q.; Wei, F.; Ma, J.; Wei, M.; Evans, D. G.; Duan, X. Hierarchical NiMn Layered Double Hydroxide/Carbon Nanotubes Architecture with Superb Energy Density for Flexible Supercapacitors. *Adv. Funct. Mater.* **2014**, No. 24, 2938–2946. https://doi.org/10.1002/adfm.201303638.

(23) Wang, B.; Williams, G. R.; Chang, Z.; Jiang, M.; Liu, J.; Lei, X.; Sun, X. Hierarchical NiAl Layered Double Hydroxide/Multiwalled Carbon Nanotube/Nickel Foam Electrodes with Excellent Pseudocapacitive Properties. *ACS Appl. Mater. Interfaces* **2014**, *6*, 16304–16311. https://doi.org/10.1021/am504530e.

(24) Khan, M.; Tahir, M. N.; Adil, S. F.; Khan, H. U.; Siddiqui, M. R. H.; Al-warthan, A.; Tremel, W. Graphene

Based Metal and Metal Oxide Nanocomposites: Synthesis, Properties and Their Application. *J. Mater. Chem. A* **2015**, *3*, 18753–18808. https://doi.org/10.1039/C5TA02240A.

(25) Gooding, J. J. Nanostructuring Electrodes with Carbon Nanotubes: A Review on Electrochemistry and Applications for Sensing. *Electrochim. Acta* **2005**, *50*, 3049–3060. https://doi.org/10.1016/j.electacta.2004.08.052.

(26) Allen, M. J.; Tung, V. C.; Kaner, R. B. Honeycomb Carbon: A Review of Graphene. *Chem. Rev.* **2010**, *110*, 132–145. https://doi.org/10.1021/cr900070d.

(27) Zhang, L.; Nam Hui, K.; San Hui, K.; Lee, H. Facile Synthesis of Porous CoAl-Layered Double Hydroxide/Graphene Composite with Enhanced Capacitive Performance for Supercapacitors. *Electrochim. Acta* **2015**, *186*, 522–529. https://doi.org/10.1016/j.electacta.2015.11.024.

(28) Wimalasiri, Y.; Fan, R.; Zhao, X. S.; Zou, L. Assembly of Ni-Al Layered Double Hydroxide and Graphene Electrodes for Supercapacitors. *Electrochim. Acta* **2014**, *134*, 127–135. https://doi.org/10.1016/j.electacta.2014.04.129.

(29) Wang, Y.; Yang, W.; Chen, C.; Evans, D. G. Fabrication and Electrochemical Characterization of Cobalt-Based Layered Double Hydroxide Nanosheet Thin-Film Electrodes. *J. Power Sources* **2008**, *184*, 682–690. https://doi.org/10.1016/j.jpowsour.2008.02.017.

(30) Scavetta, E.; Ballarin, B.; Giorgetti, M.; Carpani, I.; Cogo, F.; Tonelli, D. Electrodes Modified by One-Step Electrosynthesis of Ni/Al-NO_3 Double Layered Hydroxide. *J. New Mater. Electrochem. Syst.* **2004**, *7*, 43–50.

(31) Gualandi, I.; Monti, M.; Scavetta, E.; Tonelli, D.; Prevot, V.; Mousty, C. Electrodeposition of Layered Double Hydroxides on Platinum: Insights into the Reactions Sequence. *Electrochim. Acta* **2015**, *152*, 75–83. https://doi.org/10.1016/j.electacta.2014.11.096.

(32) Vlamidis, Y.; Scavetta, E.; Giorgetti, M.; Sangiorgi, N.; Tonelli, D. Electrochemically Synthesized Cobalt Redox Active Layered Double Hydroxides for Supercapacitors Development. *Appl. Clay Sci.* **2017**, *143*,

151–158. https://doi.org/10.1016/j.clay.2017.03.031.

(33) Basile, F.; Benito, P.; Fornasari, G.; Monti, M.; Scavetta, E.; Tonelli, D.; Vaccari, A. Novel Rh-Based Structured Catalysts for the Catalytic Partial Oxidation of Methane. *Catal. Today* **2010**, *157*, 183–190. https://doi.org/10.1016/j.cattod.2010.04.039.

(34) Gualandi, I.; Solito, A. G.; Scavetta, E.; Tonelli, D. Electrochemical Pretreatment of Pt Surface: Modification with Co/Al Layered Double Hydroxide for Analytical Applications. *Electroanalysis* **2012**, *24*, 857–864. https://doi.org/10.1002/elan.201100567.

(35) Li, M.; Cheng, J. P.; Fang, J. H.; Yang, Y.; Liu, F.; Zhang, X. B. NiAl-Layered Double Hydroxide / Reduced Graphene Oxide Composite: Microwave-Assisted Synthesis and Supercapacitive Properties. *Electrochim. Acta* **2014**, *134*, 309–318. https://doi.org/10.1016/j.electacta.2014.04.141.

(36) Zhan, T.; Zhang, Y.; Liu, X.; Lu, S.; Hou, W. NiFe Layered Double Hydroxide/Reduced Graphene Oxide Nanohybrid as an Efficient Bifunctional Electrocatalyst for Oxygen Evolution and Reduction Reactions. *J. Power Sources* **2016**, *333*, 53–60. https://doi.org/10.1016/j.jpowsour.2016.09.152.

(37) Heli, H.; Pishahang, J.; Amiri, H. B. Synthesis of Hexagonal CoAl-Layered Double Hydroxide Nanoshales/Carbon Nanotubes Composite for the Non-Enzymatic Detection of Hydrogen Peroxide. *J. Electroanal. Chem.* **2016**, *768*, 134–144. https://doi.org/10.1016/j.jelechem.2016.01.042.

(38) Li, S.; Yu, C.; Yang, J.; Zhao, C.; Zhang, M.; Huang, H.; Liu, Z.; Guo, W.; Qiu, J. A Superhydrophilic "Nanoglue" for Stabilizing Metal Hydroxides onto Carbon Materials for High-Energy and Ultralong-Life Asymmetric Supercapacitors. *Energy Environ. Sci.* **2017**, *10*, 1958–1965. https://doi.org/10.1039/c7ee01040k.

(39) Yang, B.; Yang, Z.; Wang, R.; Wang, T. Layered Double Hydroxide/Carbon Nanotubes Composite as a High Performance Anode Material for Ni–Zn Secondary Batteries. *Electrochim. Acta* **2013**, *111*, 581–587. https://doi.org/10.1016/j.electacta.2013.08.052.

(40) Zhang, X.; Wu, J.; Wang, J.; Yang, Q.; Zhang, B.; Xie, Z. Low-Temperature All-Solution-Processed

Transparent Silver Nanowire-Polymer/AZO Nanoparticles Composite Electrodes for Efficient ITO-Free Polymer Solar Cells. **2016**. https://doi.org/10.1021/acsami.6b11978.

(41) Su, L.-H.; Zhang, X.; Liu, Y. Electrochemical Performance of Co–Al Layered Double Hydroxide Nanosheets Mixed with Multiwall Carbon Nanotubes. *J. Solid State Chem.* **2008**, *12*, 1129–1134. https://doi.org/10.1007/s10008-007-0455-5.

(42) Kudinalli, L.; Bhatta, G.; Subramanyam, S.; Chengala, M. D.; Bhatta, U. M.; Guha, P.; Prasad, R.; Dinakar, H.; Venkatesh, K. Layered Double Hydroxides/Multiwalled Carbon Nanotubes-Based Composite for High-Temperature CO_2 Adsorption. **2016**. https://doi.org/10.1021/acs.energyfuels.6b00141.

(43) Sharma, V. V.; Gualandi, I.; Vlamidis, Y.; Tonelli, D. Electrochemical Behavior of Reduced Graphene Oxide and Multi-Walled Carbon Nanotubes Composites for Catechol and Dopamine Oxidation. *Electrochim. Acta* **2017**, *246*. https://doi.org/10.1016/j.electacta.2017.06.071.

(44) McCrory, C. C. L.; Jung, S.; Ferrer, I. M.; Chatman, S. M.; Peters, J. C.; Jaramillo, T. F. Benchmarking Hydrogen Evolving Reaction and Oxygen Evolving Reaction Electrocatalysts for Solar Water Splitting Devices. *J. Am. Chem. Soc.* **2015**, *137*, 4347–4357. https://doi.org/10.1021/ja510442p.

(45) Bard, A. J.; Faulkner, L. R. *Electrochemical Methods, Fundamentals and Applications*, Second.; Wiley: New York, US, 2000.

(46) Pournaghi-Azar, M. H.; Razmi-Nerbin, H. Electrocatalytic Characteristics of Thiosulfate Oxidation at Nickel Plated Aluminum Electrode Modified with Nickel Pentacyanonitrosylferrate Films. *J. Electroanal. Chem.* **2000**, *488*, 17–24. https://doi.org/10.1002/1521-4109(200104)13:6<465::AID-ELAN465>3.0.CO;2-Q.

(47) De Groot, M. T.; Koper, M. T. M. The Influence of Nitrate Concentration and Acidity on the Electrocatalytic Reduction of Nitrate on Platinum. *J. Electroanal. Chem.* **2004**, *562*, 81–94. https://doi.org/10.1016/j.jelechem.2003.08.011.

(48) Boclair, J. W.; Braterman, P. S. Layered Double Hydroxide Stability. 1. Relative Stabilities of Layered

Double Hydroxides and Their Simple Counterparts. *Chem. Mater.* **1999**, *11*, 298–302. https://doi.org/10.1021/cm980523u.

(49) Boclair, J. W.; Braterman, P. S.; Jiang, J.; Lou, S.; Yarberry, F. Layered Double Hydroxide Stability. 2. Formation of Cr(III)-Containing Layered Double Hydroxides Directly from Solution. *Chem. Mater.* **1999**, *11*, 303–307. https://doi.org/10.1021/cm980524m.

(50) Hoang Ho, P.; Monti, M.; Scavetta, E.; Tonelli, D.; Bernardi, E.; Nobili, L.; Fornasari, G.; Vaccari, A.; Benito, P. Reactions Involved in the Electrodeposition of Hydrotalcite-Type Compounds on FeCrAlloy Foams and Plates. *Electrochim. Acta* **2016**, *222*, 1335–1344. https://doi.org/10.1016/j.electacta.2016.11.109.

(51) Scavetta, E.; Berrettoni, M.; Seeber, R.; Tonelli, D. [Ni/Al-Cl]-Based Hydrotalcite Electrodes as Amperometric Sensors: Preparation and Electrochemical Study. *Electrochim. Acta* **2001**, *46*, 2681–2692. https://doi.org/10.1016/S0013-4686(01)00487-X.

(52) Scavetta, E.; Casagrande, A.; Gualandi, I.; Tonelli, D. Analytical Performances of Ni LDH Films Electrochemically Deposited on Pt Surfaces: Phenol and Glucose Detection. *J. Electroanal. Chem.* **2014**, *722–723*, 15–22. https://doi.org/10.1016/j.jelechem.2014.03.018.

(53) Guo, W.; Yu, C.; Li, S.; Yang, J.; Liu, Z.; Zhao, C.; Huang, H.; Zhang, M.; Han, X.; Niu, Y.; Qiu, J. High-Stacking-Density, Superior-Roughness LDH Bridged with Vertically Aligned Graphene for High-Performance Asymmetric Supercapacitors. *Small* **2017**, *13*, 1–9. https://doi.org/10.1002/smll.201701288.

(54) Gualandi, I.; Scavetta, E.; Vlamidis, Y.; Casagrande, A.; Tonelli, D. Co/Al Layered Double Hydroxide Coated Electrode for in Flow Amperometric Detection of Sugars. *Electrochim. Acta* **2015**, *173*, 67–75. https://doi.org/http://dx.doi.org/10.1016/j.electacta.2015.04.172.

(55) Sinha, L.; Pakhira, S.; Bhojane, P.; Mali, S.; Hong, C. K.; Shirage, P. M. Hybridization of Co_3O_4 and α-MnO2Nanostructures for High-Performance Nonenzymatic Glucose Sensing. *ACS Sustain. Chem. Eng.*

2018, *6*, 13248–13261. https://doi.org/10.1021/acssuschemeng.8b02835.

(56) Fu, S.; Fan, G.; Yang, L.; Li, F. Non-Enzymatic Glucose Sensor Based on Au Nanoparticles Decorated Ternary Ni-Al Layered Double Hydroxide/Single-Walled Carbon Nanotubes/Graphene Nanocomposite. *Electrochim. Acta* **2015**, *152*, 146–154. https://doi.org/10.1016/j.electacta.2014.11.115.

(57) Wang, F.; Zhang, Y.; Liang, W.; Chen, L.; Li, Y.; He, X. Non-Enzymatic Glucose Sensor with High Sensitivity Based on Cu-Al Layered Double Hydroxides. *Sensors Actuators B. Chem.* **2018**, *273*, 41–47. https://doi.org/10.1016/j.snb.2018.06.038.

(58) Zhou, J.; Min, M.; Liu, Y.; Tang, J.; Tang, W. Layered Assembly of NiMn-Layered Double Hydroxide on Graphene Oxide for Enhanced Non-Enzymatic Sugars and Hydrogen Peroxide Detection. *Sensors Actuators B. Chem.* **2018**, *260*, 408–417. https://doi.org/10.1016/j.snb.2018.01.072.

(59) Wang, X.; Zheng, Y.; Yuan, J.; Shen, J.; Hu, J.; Wang, A. J.; Wu, L.; Niu, L. Three-Dimensional NiCo Layered Double Hydroxide Nanosheets Array on Carbon Cloth, Facile Preparation and Its Application in Highly Sensitive Enzymeless Glucose Detection. *Electrochim. Acta* **2017**, *224*, 628–635. https://doi.org/10.1016/j.electacta.2016.12.104.